Chemistry and Physics of Lipids 221 (2019) 73–82

Contents lists available at ScienceDirect

Chemistry and Physics of Lipids

journal homepage: www.elsevier.com/locate/chemphyslip

Functional characterization of anti-cancer sphingolipids from the marine crab *Dromia dehanni*

Elangovan RethnaPriya[a], Samuthirapandian Ravichandran[a,*], Thilagar Gobinath[a], Supriya Tilvi[b], S. Prabha Devi[b]

[a] Centre of Advanced Study in Marine Biology, Faculty of Marine Sciences, Annamalai University, Parangipettai, 608 502, India
[b] CSIR-National Institute of Oceanography, 403 004, Dona Paula, Goa, India

ARTICLE INFO

Keywords:
Crab
Dromia dehanni
Hemolymph
Anticancer compounds
Sphingolipid
NDEA in rat model

ABSTRACT

Sphingolipids have been considered for many years only as structural components of membranes. It is now acknowledged that they are also involved in controlling cellular processes such as proliferation.The present work was designed to find the anticancer activity of the crab *Dromia dehanni* hemolymph in *in-vivo* and in vitro with special reference to the anticancer compound sphingolipids isolation and characterization. The active fraction of the purified hemolymph was subjected to NMR and ESI-MS/MS analysis. The ESI-MS/MS spectrum exhibited intense signals for sodiated molecular ions $[M + Na]^+$ of sphingomyelins (SM) identified as *N*-2-O-Acetyl-12 pentadecenoyl sphingosine phosphorylcholine, *N*-9-eicosenoyl- sphinganine phosphocholine and the corresponding dehydro sphingomyelin, *N*-9-eicosenoyl- dehydro- sphinganine phosphocholine along with the ions at *m/z* 147, 184 characteristic of phosphocholine. The present study revealed *D. dehaani* might be a great source for the novel anti-cancer compounds which can be used for human benefits.

1. Introduction

Sphingolipids have emerged as bio effector molecules, controlling various aspects of cell growth and proliferation in cancer, which is becoming the deadliest disease in the world. These lipid molecules have also been implicated in the mechanism of action of cancer chemotherapeutics. Sphingolipids have been considered for many years only as structural components of membranes. However, it is now acknowledged that they are also involved in controlling cellular processes such as, differentiation (Zhang et al., 2003), migration (Padrón, 2006), apoptosis (Morales et al., 2007), growth (Ponnusamy et al., 2010), proliferation (Pitson, 2011) and senescence (Trayssac et al., 2018). Sphingolipids are the bioactive compound and an anti-cancer drug against many malignancies like intestinal cancer, cervical cancer (De Luca et al., 2010), Prostate Cancer (Symolon et al., 2011), and colon cancers (García-Barros et al., 2014).

After the first recognition of sphingolipids in 1970's (Atkinson et al., 2010), numerous sphingolipids have been isolated from various marine organisms such as, soft corals (Dmitrenok et al., 2003), algae (Khotimchenko and Vas'kovsky, 2004), sea cucumber (Sugawara et al., 2006), sponges (Ayyad et al., 2009), and tunicates (Jr, 2011). However, there is very limited study on anticancer sphingolipids from brachyuran crabs. Keeping this in mind, the primary objective of the present work was designed to find the anticancer activity of the crab *D. dehaani* hemolymph in in vivo and in vitro (NDEA in rat model)with the special reference to the anti-cancer compound sphingolipids isolation and characterization.

2. Materials and methods

2.1. Animal and sample collection

Marine crabs *D. dehaani* (200–250 g) were collected from the Pazhayar landing center (11°21′16.8415″N-79°49′38.6512″E, Southeast coast of India). They were cultured in 500 L recirculating seawater (20–30%) tanks at the laboratory for two weeks before the starting of the experiments. They were fed twice daily with the control diet and 50% of the water was exchanged daily thrice in a week to maintain the water quality. Hemolymph was collected by cutting walking legs of the crab *D. dehaani* with fine sterile scissors. To avoid hemocyte degranulation and coagulation, the hemolymph was collected in the presence of sodium citrate buffer, pH 4.6 (2:1, V/V). An equal volume of physiological saline (0.85%, NaCl, w/v) was added to it (Jayanthi et al., 2017). To remove hemocytes from the hemolymph, it was

* Corresponding author.
E-mail address: sravicas@gmail.com (S. Ravichandran).

https://doi.org/10.1016/j.chemphyslip.2019.03.010
Received 25 November 2018; Received in revised form 21 March 2019; Accepted 21 March 2019
Available online 25 March 2019

centrifuged at 2000 RPM for 15 min at 4 °C. The supernatant was collected by aspirating and stored at 4 °C until use.

2.2. In-vivo anticancer activity

Male albino Wistar rats (180–200 g) obtained from the Central Animal House, Department of Experimental Medicine, Rajah Muthiah Medical College, Annamalai University, and maintained in an air-conditioned room (25 ± 3 °C) with a 12-h light:12-h dark cycle. Ad libitum Food (Pranav Agro Industries Ltd., Maharashtra, India and water were provided to all the animals. All studies conducted in accordance with the National Institute of Health Guide for the Care and Use of Laboratory Animals and the study was approved by the Ethical Committee of Rajah Muthiah College and Hospital (Reg. No. 1038/2013/CPCSEA), Annamalai University, Annamalainagar.

2.3. Chemicals and tumor induction

Nitrosodiethylamine (NDEA) was purchased from Sigma-Aldrich Chemicals Co. Hepatocellular carcinoma was induced in male Wistar rats by providing 0.01% of NDEA through drinking water for 15 weeks (Ramakrishnan et al., 2008).

2.4. Hemolymph preparation

Hemolymph was dissolved in saline and each rat received daily 1 mL at a dose of 40 mg/kg body weight orally by intra gastric intubation throughout the experimental period (Schock et al., 2010).

2.5. Processing of blood and tissue samples

2.5.1. Serum preparation

Blood was collected in a dry test tube and allowed to coagulate at ambient temperature for 30 min. Serum was separated by centrifugation at 3000 rpm for 15 min(Yao et al., 2017).

2.5.2. Plasma preparation

The blood collected in a heparinized centrifuge tube was centrifuged at 2000 rpm for 10 min and the plasma was separated by aspiration, transferred into tubes and stored at -4 °C until analysis.

2.5.3. Erythrocyte preparation

After the separation of plasma, the buffy coat, enriched in white cells, was removed and the remaining erythrocytes were washed three times with physiological saline. A known volume of erythrocyte was lysed with hypotonic phosphate buffer at pH 7.4. The hemolysate was separated by centrifugation at 2500 rpm for 10 min and the supernatant was used for the estimation of enzymatic antioxidants.

2.5.4. Tissue homogenate preparation

Liver and kidney tissues (250 mg) were cut into pieces and homogenized in appropriate buffer in cold condition (pH 7.0) to give 20% homogenate (w/v). The homogenate were centrifuged at 1000 rpm for 10 min at 0 °C in cold centrifuge. The supernatant was separated and used for various biochemical estimations.

2.5.5. Tissue sampling for histopathological study

For histopathological study, three rats from each group were perfused with cold physiological saline, followed by formalin (10% formaldehyde). The liver and kidney were excised immediately and fixed in 10% formalin.

2.6. Histopathological examination

After fixation of the liver portion of rats in the studied groups in formal saline (10%) for 24 h, the tissues were then washed in running tap water, dehydrated in series of alcohol (methyl, ethyl and absolute alcohol). The specimens were cleared in xylene and embedded in paraffin at 56 ° in hot air oven for twenty four hours. The paraffin bees wax tissue blocks were sectioned by rotatory microtome at thickness of 4 µm. The obtained tissue sections were collected on clean glass slides and left in the oven at 40 °C for dryness. The slides were deparaffinized in xylene and then immersed in descending series of alcohol, stained by hematoxylin and eosin stain then examined using light electric microscope (Karthick et al., 2016).

2.7. Preparation of the sample

The buffered sample of hemolymph was passed through sephadex LH-20 and eluted with methanol. The fraction designated as fraction R5 was found to show the presence of organic components. Hence, it was purified further and subjected to spectral analysis. The sphingolipids from the hemolymph were identified using following methods.

2.8. Spectral analysis of fraction R5

Electrospray ionization tandem mass spectrometry (ESI-MS/MS), a highly sensitive and selective technique, was applied for the analysis of unprocessed (Chen, 2003) cellular lipid extract. The identification is based on their characteristic *m/z* values, fragmentation analysis and headgroup, specific neutral loss or precursor ion. As the fragmentation of similar structures follows similar pathways, the mass of the protonated/sodiated molecule and its fragmentation pattern readily lead to the unambiguous identification of a polar lipid.

2.9. ESI-QTOF MS/MS spectrometry

Mass spectra were recorded on an electrospray ionization -quadrupole time-of-flight (ESI-QTOF)-QSTAR XL MS/MS, Applied Biosystems instrument equipped with MDS Sciex Analyst Software (Concord Ontario, Canada). The instrument was used either in the single stage MS mode or in the tandem MS mode to yield diagnostic product ion mass spectra, which were characteristic of the structural moieties present in the analyte. The collision energy (CE) varied from 20 to 60 v so as to obtain optimum fragmentation. The extract after dilution with 1:1 (MeOH: H_2O) were directly infused, at a flow rate of 10 µl/min into the ion spray source by means of a Harvard syringe pump.

2.10. Nuclear magnetic resonance (NMR)

Nuclear Magnetic Resonance (NMR) spectra of the sample were obtained in $CDCl_3$ on a Bruker Avance (300 MHz) instrument with TMS as the internal standard.

3. Results

3.1. In vivo anticancer activity

The total number and size of nodules in experimental animals were shown in Table 1. The hemolymph treated group - 4 showed a significant decrease in the number and size nodules when compared with 3rd group animals. Animals treated with NDEA showed an increased the relative liver weight to body weight compared to the group - 1. However, administration of the hemolymph to group four significantly reduced the relative liver weight compared to group - 3 animals.

Table 2 shows the body and liver weights of control and experimental animals. The body weights were significantly decreased in NDEA-treated animals as compared with control. Treatment of hemolymph to NDEA-treated rats significantly improved the body weight as compared to group 3 animals. The schematic representation of rat liver of control and experimental animals has shown in Fig. 1.

Table 1
Effect of hemolymph on number, size of nodules and tumor incidence in control and experimental animals.

	Control	Hemolymph	NDEA	NDEA + hemolymph
Tumor incidence	–	–	6/6	2/6
Total number no of nodules	–	–	104*	52**
Average number of nodules/nodules bearing liver	–	–	16.09 ± 1.3*	8.27 ± 0.3**
Relative size (% of total numbers)				
< 1 mm	–	–	52 (49.2)	30 (54.1)
> 1 mm < 3 mm	–	–	32 (30.3)	15(29.7)
> 3 mm	–	–	18 (17.5)	7 (11.1)

*Significantly different from control $p < 0.001$ ANOVA followed by DMRT.
*Significantly different from group 3 $p < 0.001$ ANOVA followed by DMRT.

3.2. Histopathological changes

The pictorial representation of the different stages of liver was presented in Fig. 2. Histopathological examinations of the present examination fundamentally support the results obtained from serum enzyme and tumor marker assays are shown in Fig. 2. It demonstrates the normal architecture (Control) and cells cytoplasm of hepatic cells with granulated cytoplasm, central vein, small uniform nuclei and nucleolus (Fig. 2a). Hemolymph treated animals showed normal architecture illustrating the non-toxic nature of hemolymph (Fig. 2b). NDEA alone (Fig. 2c) showed loss of architecture and tumor cells which were smaller than normal cells with granular cytoplasm and large hyper chromatic nuclei, whereas group - 4 animals pretreated with hemolymph showed few neoplastically transformed cells and hepatocytes maintaining near normal architecture (Fig. 2d).

3.3. Nuclear magnetic resonance (NMR)

The proton NMR spectrum (Fig. 3) of sphingolipid fraction (R5) exhibited signals at δ 5.36 and 5.35 for the unsaturation and δ4.32, 4.14, 3.96, 3.72, 3.48, 3.26 for methine and methylene protons next to oxygen/nitrogen. The signal at δ2.02 is due to acetyl methyl and the long polymethylene chain and the terminal methyl group were evident from the signals between δ 1–1.6 and δ 0.88 respectively.

^{13}CNMR (Fig. 4) of the samples R-5 is also in agreement for the presence of carbonyl group (173.3 ppm) as well as unsaturation (cluster of signals with the most intense signal at 129.9 ppm). The signal at 54.38 ppm was due to methylene next to nitrogen. Methylene adjacent to oxygen are also present but the intensity is low due to low concentration of the components.

3.4. ESI-QTOF MS/MS spectrometry

Fig. 5, shows ESI-MS of hemolymph (R5) of brachyuran crab in the positive ion mode. It gave the most abundant signal at *m/z* 228 and 206 corresponding to di- and *m/z* 206 monosodium salt of phosphocholine respectively. In addition to this it also showed peaks in the mas range *m/z* 700-850. To characterize structure of the compounds, the individual peaks were subjected to tandem mass spectrometry (MS/MS). Tandem mass spectrum of disodium salt at *m/z* 228 (Fig. 6) yielded fragments which were well in agreement with the structure. The fragment ions are represented in the Fig. 7.

Collision induced dissociation mass spectrum of $[M + Na]^+$ ion of acetylated sphingomyelin at *m/z* 810 is shown in Fig. 8 It exhibited base peak (100%) at *m/z* 147 due to sodiated fragment derived from phosphocholine on elimination of trimetylamine and the signal at *m/z* 184 due to phosphocholine itself. The signal at *m/z* 627 corresponded to the loss of polar choline phosphate head group as a neutral fragment of 183 Da from the sodiated sphingomyelin molecule, while the ion at 605 results from the loss of sodium atom from the fragment at *m/z* 627. In addition, the ion observed at *m/z* 751 results from the loss of $[N(CH_3)_3]$ moiety from the choline phosphate head group of the molecule (Fig. 8).

CID-MS of ion at $[M + Na]^+$ at *m/z* 782 is as shown in Fig. 8. The polar head group (PHG) of sphingolipid with $[M + Na]^+$ at *m/z* 782 was deduced to be phosphocholine on the basis of neutral loss of trimethyl amine/ PC moiety from the molecule (fragments at *m/z* 723/599). The signal at *m/z* 577 corresponded to the loss of sodium atom from the fragment at *m/z* 599. The presence of the most intense signal at *m/z* 147 and *m/z* 86 further confirmed phosphocholine as the PHG. Based on foregoing fragmentation observed, the identity of SM was established as *N*-9-eicosenoyl- sphinganine phosphorylcholine (Fig. 9). Similarly, sodiated molecular ion $[M + Na]^+$ at *m/z* 754 is 18 amu less than the molecular mass of compound which indicated that it was dehydrated sphingomyelin (Fig. 8) and it was assigned structure. The fragmentation observed in tandem mass spectrum of sodiated molecular ion $[M + Na]^+$ at *m/z* 754 (Fig. 8) is well in agreement with *N*-9-eicosenoyl-dehydro-sphinganine phosphocholine, Thus, elimination of neutral molecule of trimethylamine from the sphingomyeline with sodiated molecular ion $[M + Na]^+$ at *m/z* 754 yielded a signal at *m/z* 695 while cleavage leading to the loss of neutral molecule of phosphocholine (183amu) followed by loss of sodium atom gave peaks at *m/z* 571 and *m/z* 549 respectively. Signals at *m/z* 86, 123, and 147 are characteristic of phosphocholine moiety.

4. Discussion

4.1. In vivo anticancer activity

An understanding of how cancer can be prevented is one of the key intentions of the modern research. Hepato-carcinogenesis is a long-

Table 2
Body weight, organ weight, food and water intake in control and experimental rats.

Groups	Body weight (g)		Food and Water intake		Organ weight
	Initial	Final	Food intake (g/100 g bw /day)	Water intake (mL/rat/day)	Liver
Control	150 ± 20.00	290 ± 18.09	6.3 ± 0.5	11.1 ± 4.5	7.65 ± 0.61
Hemolymph	156 ± 19.50	296 ± 19.80	6.1 ± 0.4	11.9 ± 3.1	7.60 ± 0.63
NDEA	165 ± 16.00*	190 ± 12.00*	2.8 ± 0.2*	5.9 ± 3.2*	11.00 ± 1.01*
NDEA + Hemolymph	160 ± 17.55**	229 ± 17.03**	5.9 ± 0.3**	10.6 ± 4.1**	8.63 ± 0.69**

* Significantly different from control $p < 0.001$ ANOVA followed by DMRT.
** Significantly different from group 3 $p < 0.001$ ANOVA followed by DMRT.

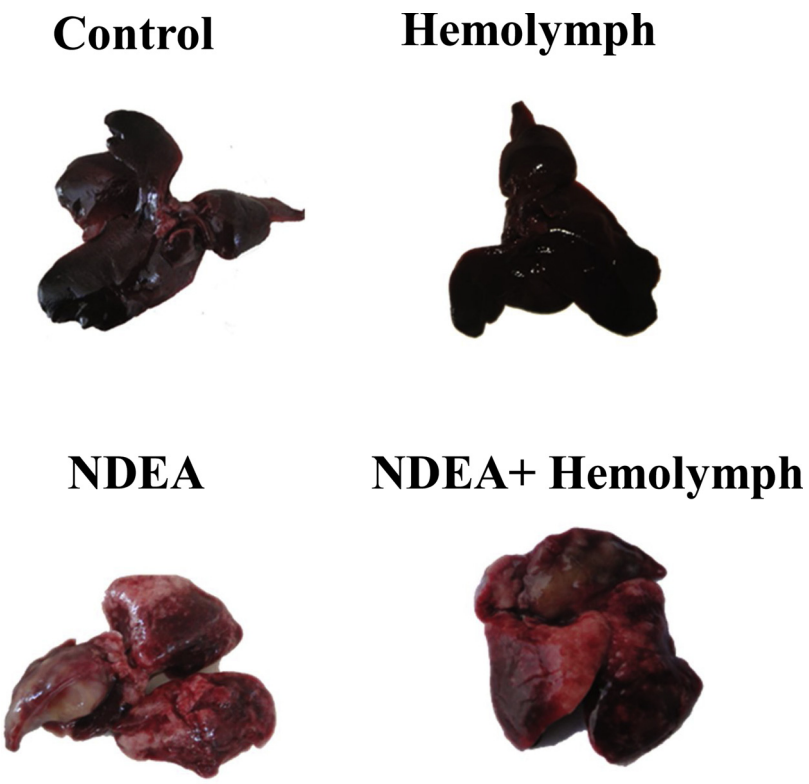

Fig. 1. Pictographic image of liver (Control image shows normal liver, hemolymph alone treated rats shows similar like control, NDEA treated livers shows tumor developed liver and NDEA + hemolymph treated liver shows Nearby control liver.).

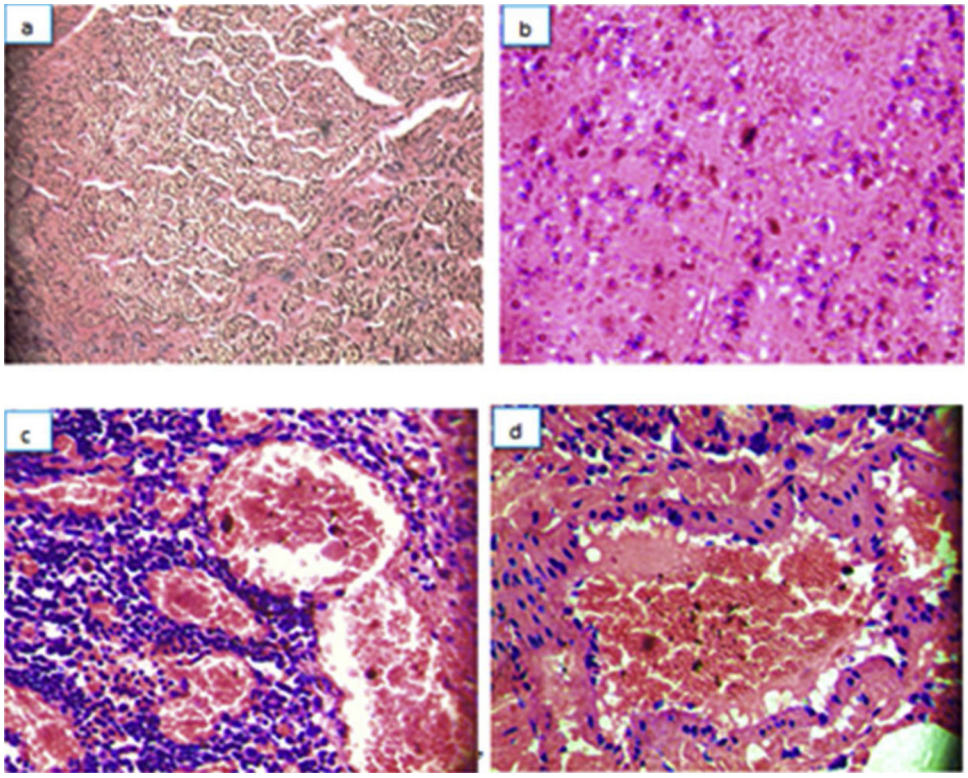

Fig. 2. Histopathological changes of liver in control and experimental rats (a) Liver tissue of the normal group (control) showed hepatic lobule having normal architecture (40x, HE). (b) Liver tissue of the hemolymph treated group showed hepatic lobule having normal architecture (40x, HE). (c) NDEA alone showing loss of architecture, mitotic, granular cytoplasm and neoplastic cells. (d) Few neoplastically transformed cells and hepatocytes maintaining near normal architecture observed in hemolymph (40×, HE) mice.

term, multistage process with the involvement of multiple risk factors (Linhart et al., 2014). Chemical exposure is one of these important risk factors causing Hepatocellular carcinoma (HCC), 2-nitropropane (2-NP) as a hepatocarcinogen was denitrified to nitrite and acetone by liver microsomes, This metabolic activation was responsible for the hepatotoxicity of 2-NP due the resulting reactive oxygen species which led to cellular damage(Abdel-Mawla et al., 2013). In the present study, mice hepatocellular carcinoma had been induced by NDEA. It showed variable histopathological changes with respect to the period of exposure.

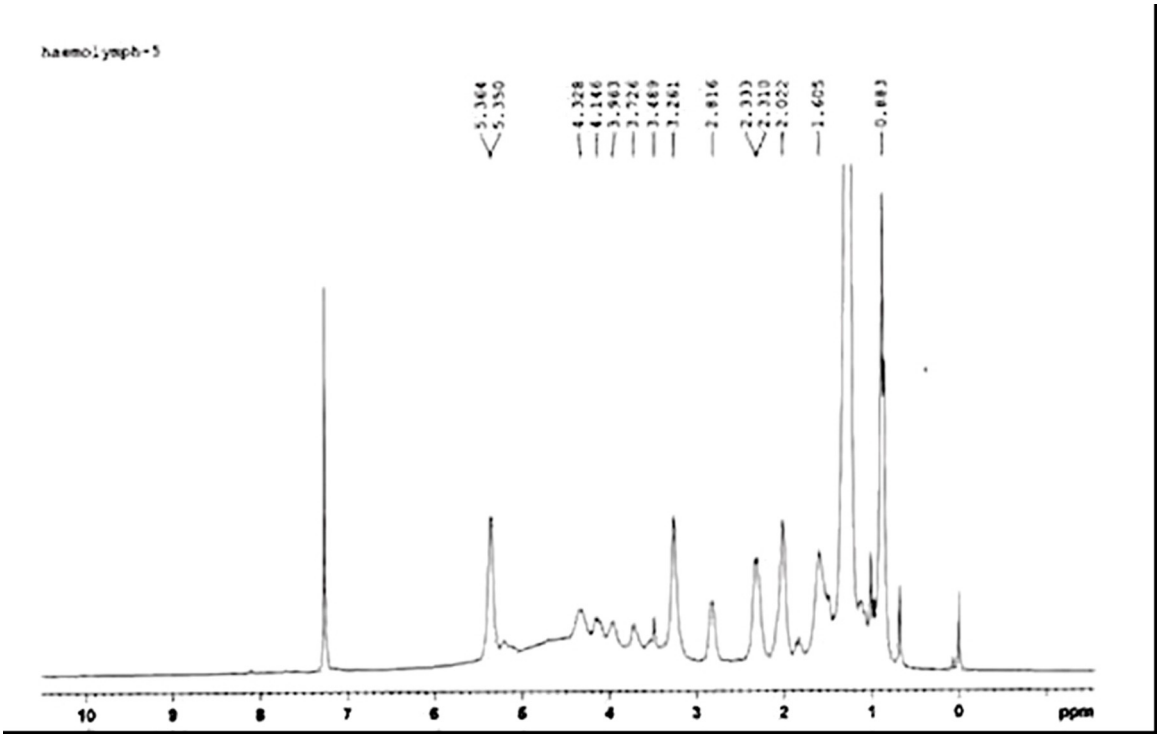

Fig. 3. ^{1}H NMR spectrum in $CDCl_3$ of hemolymph fraction R5 of brachyuran crab.

Nitrosamines are known as pre carcinogens capable of inducing tumors in different animal species and are suspected of being involved in some human tumors (Trafalis et al., 2010). *N*-Nitrosodiethylamine (NDEA), which is present in the environment and in tobacco smoke, and is also synthesized endogenously (Ali et al., 2014). NDEA is known as precarcinogen capable of inducing tumors in different animal species and are suspected of being involved in some human tumors (Balamurugan and Karthikeyan, 2012). The present findings were

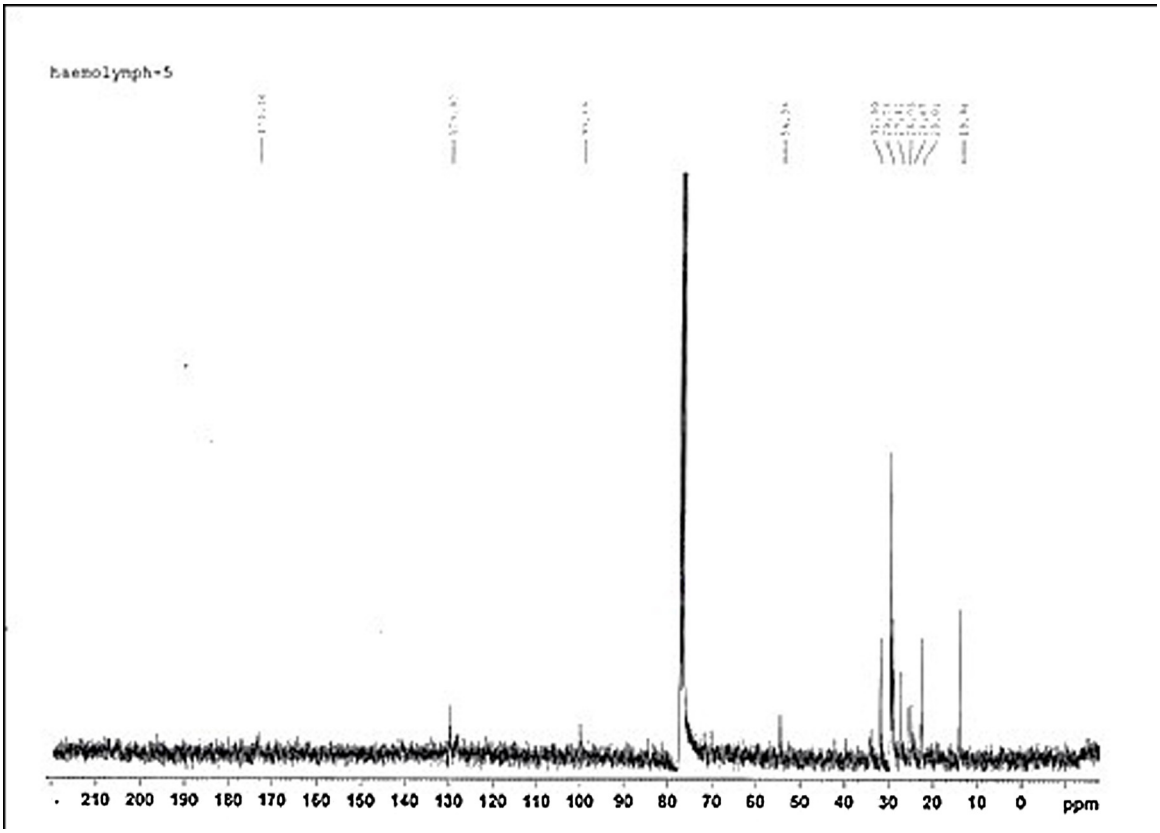

Fig. 4. ^{13}CNMR spectrum in $CDCl_3$ of hemolymph fraction R5 of brachyuran crab.

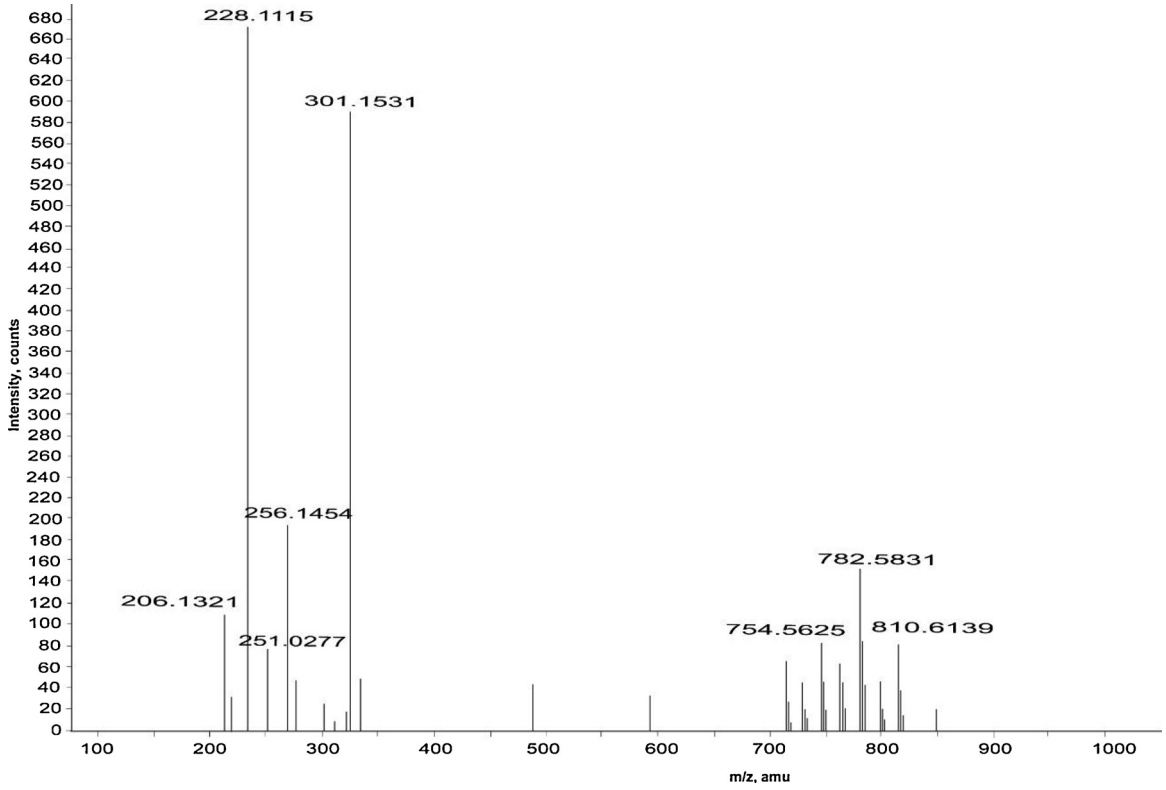

Fig. 5. ESI-MS profile of hemolymph fraction R-5 of brachyuran crab.

confirming results reported that administration of NDEA to rats resulted in lipid peroxidation (represented in higher MDA levels) and enhanced chemiluminescence in liver preneoplastic nodules, indicating the formation of activated oxygen species (Wu et al., 2010).

Chemical induction of liver carcinogenesis in rats initiated by the potent hepatocarcinogen NDEA has been considered as one of the most

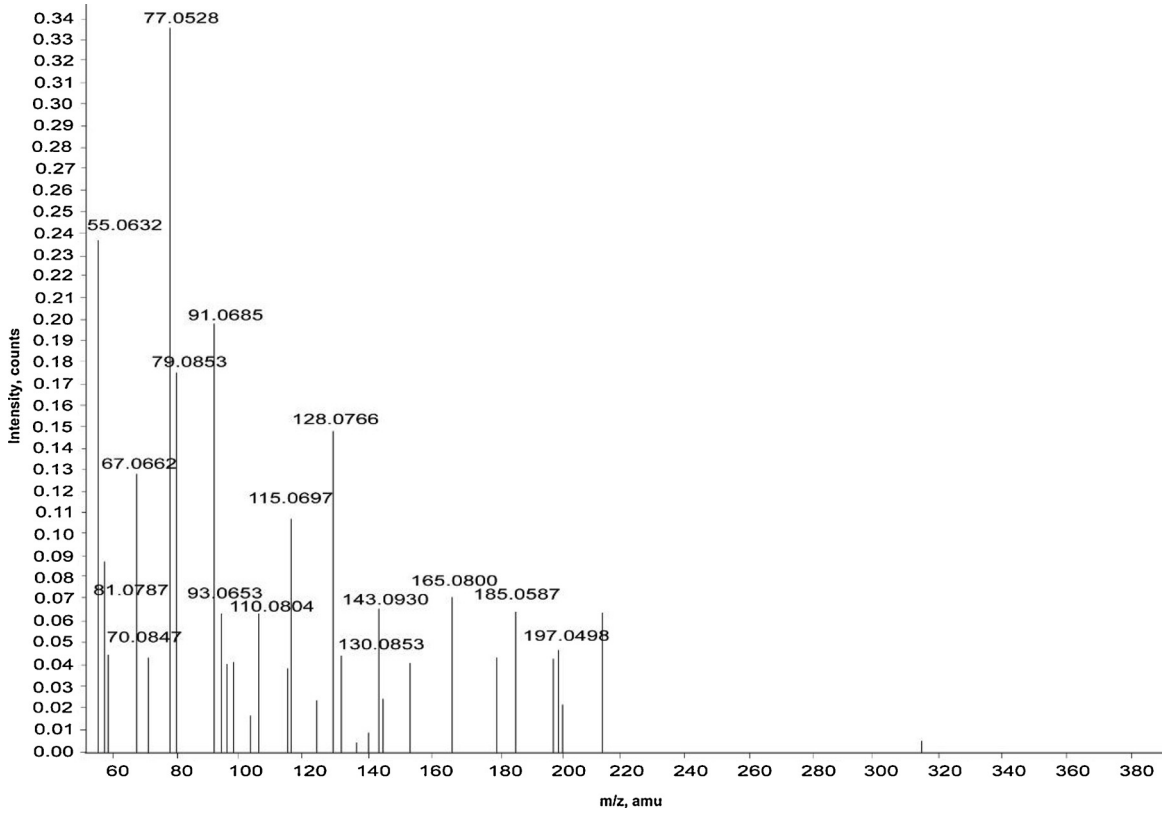

Fig. 6. MS/MS spectrum of disodium salt of phosphocholine at *m/z* 228.

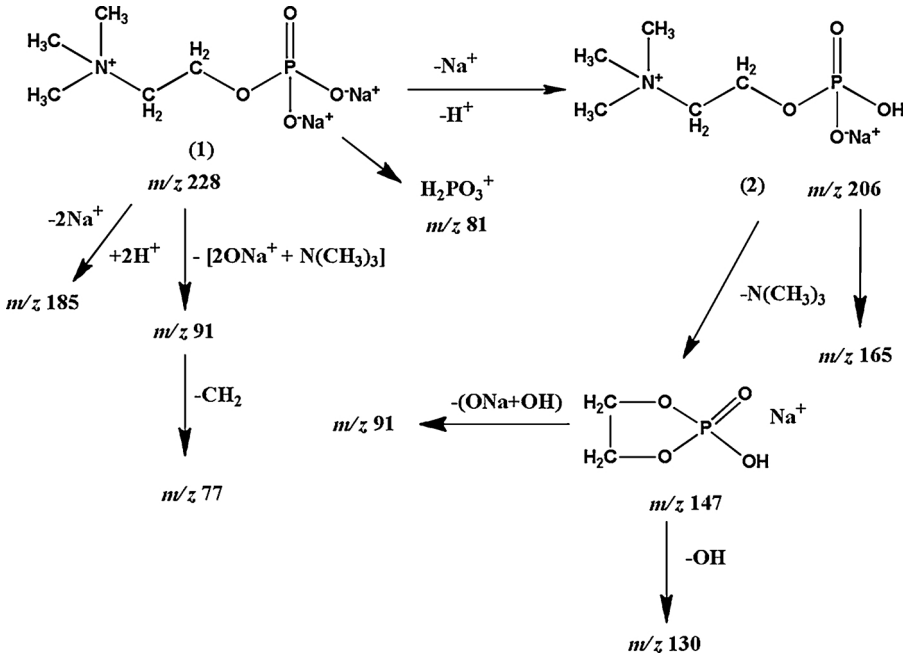

Fig. 7. Fragmentation of disodium salt of phosphocholine.

accepted and widely used experimental model that closely mimics a subclass of human HCC to study hepato-carcinogenesis and to allow screening of potential anti-cancer agents on various phases of neoplastic disease (Hoshida et al., 2014). It has long been recognized that exposure of rats to certain carcinogens like NDEA causes an elevation of circulating AFP levels. The up regulation of AFP gene expression in NDEA in toxicated rats might be due to necrosis of hepatocytes caused by NDEA. Hepatocyte localization within or outside the liver plate is the defining factor that regulates the activity of AFP synthesis on a cellular level (Arul and Subramanian, 2013).

Histopathological examination of liver tissue of HCC group showed inflammatory cells infiltration and fibroblastic cells proliferation that divide the cancer and necrosed hepatocytes of the parenchyma into nodules with hyperchromatic nuclei as well as cellular pleomorphism and polarity. These remarkable features of hepatocellular carcinoma are in agreement with the studies of (Piana et al., 2011)Liver tissue obtained from HCC group treated with NDEA revealed focal areas of hyperplasia with fibrosis and inflammatory cells infiltration. These results are partially consistent with the results of (Ahmed et al., 2013) who demonstrated that the treatment of rats, exposed to thioacetamide, with low dose of carvacrol shows mild architectural damage, less sinusoidal congestion, and less inflammatory cell infiltration. While the liver sections obtained from rats that received hemolymph only (control group) showed normal architecture which confirms that hemolymph did not induce any intracellular morphology of liver cell. This eventually shows its nontoxic nature at the given dosage. Conclusively, the histopathological data reported here suggest that the marine crab *D. dehaani* hemolymph has anticancer potential due to its ability to block the carcinogenic effect of NDEA. Hence to confirm the compounds present in the hemolymph which is responsible for its anticancer activity was further analyzed by the various spectral analyses.

4.2. Characterization of anti-cancer sphingolipids

The present study is carried out to evaluate the purification and functional characterization of the sphingolipid from the hemolymph of the sponge crab *D. dehaani*. Marine invertebrates rely solely on innate immune mechanisms that include both humoral and cellular responses (Divya et al., 2018; Gowda et al., 2008; Rekha et al., 2018). In the current research tandem mass spectrum of disodium salt yielded fragment which were well in agreement with the structure and the spectrum also exhibited intense signals for sodiated molecular ions [M + Na]+ of sphingomyelins (SM) identified as *N*-2-O-Acetyl-12 pentadecenoyl sphingosine phosphorylcholine (3, *m/z* 809), *N*-9-eicosenoyl- sphinganine phosphocholine (4, *m/z* 782) and the corresponding dehydro sphingomyelin, *N*-9-eicosenoyl- dehydro- sphinganine phosphocholine (5, *m/z* 754) along with the ions at *m/z* 147, 184 characteristic of phosphocholine (Reis et al., 2004). Sphingolipid metabolism produces second messengers as ceramide, sphingosine and sphingosine-1-phosphate which have different functions in cell life. For instance, while ceramide can mediate and induce cell death, sphingosine-1- phosphate results to be a second messenger for cell survival and proliferation and protection against ceramide mediated apoptosis (Spiegel and Kolesnick, 2002).

Sphingolipid-based second messengers, including ceramide-1-phosphate and glycol-sphingolipids are also in dynamic flux with ceramide. Thus, pharmacological or molecular manipulations of any of the enzymes involved in SL metabolism have been proposed as a tool to increase the sensitivity of tumors to various therapeutic agents (Fox et al., 2006). We have identified daughter fragments of the sodiated adduct of acetylated sphingomyelin at *m/z* 809. In the current study, the tested hemolymph gave the most abundant signal at *m/z* 228 corresponding to the disodium salt of phosphocholine and the ion corresponding to the monosodium salt of phosphocholine at *m/z* 206. Fragmentation observed in the CID spectrum is consistent with the structure of *N-2-O*-acetyl-12 pentadecenoyl acetyl sphingosine phosphorylcholine reported as biologically active phospholipid exhibiting PAF-like activity in cyanobacteria *Scytonemajulianum* (Antonopoulou et al., 2002).The fragmentation observed in the CID spectrum is consistent with the structure of *N*-2-O-acetyl-12 pentadecenoyl acetyl sphingosine phosphorylcholine reported as biologically active phospholipid exhibiting PAF-like activity in cyanobacteria *Scytonemajulianum* (Antonopoulou et al., 2002).

In recent years, a variety of natural products from marine samples have shown a wide spectrum of biological activities and numerous therapeutic applications including antiviral, antibacterial, and antitumor activities. Cyclic and linear peptides discovered from marine animals have increased our knowledge about new potent cytotoxic, antimicrobial, ion channel specific blockers, as well as several other properties with where novel chemical structures have been associated

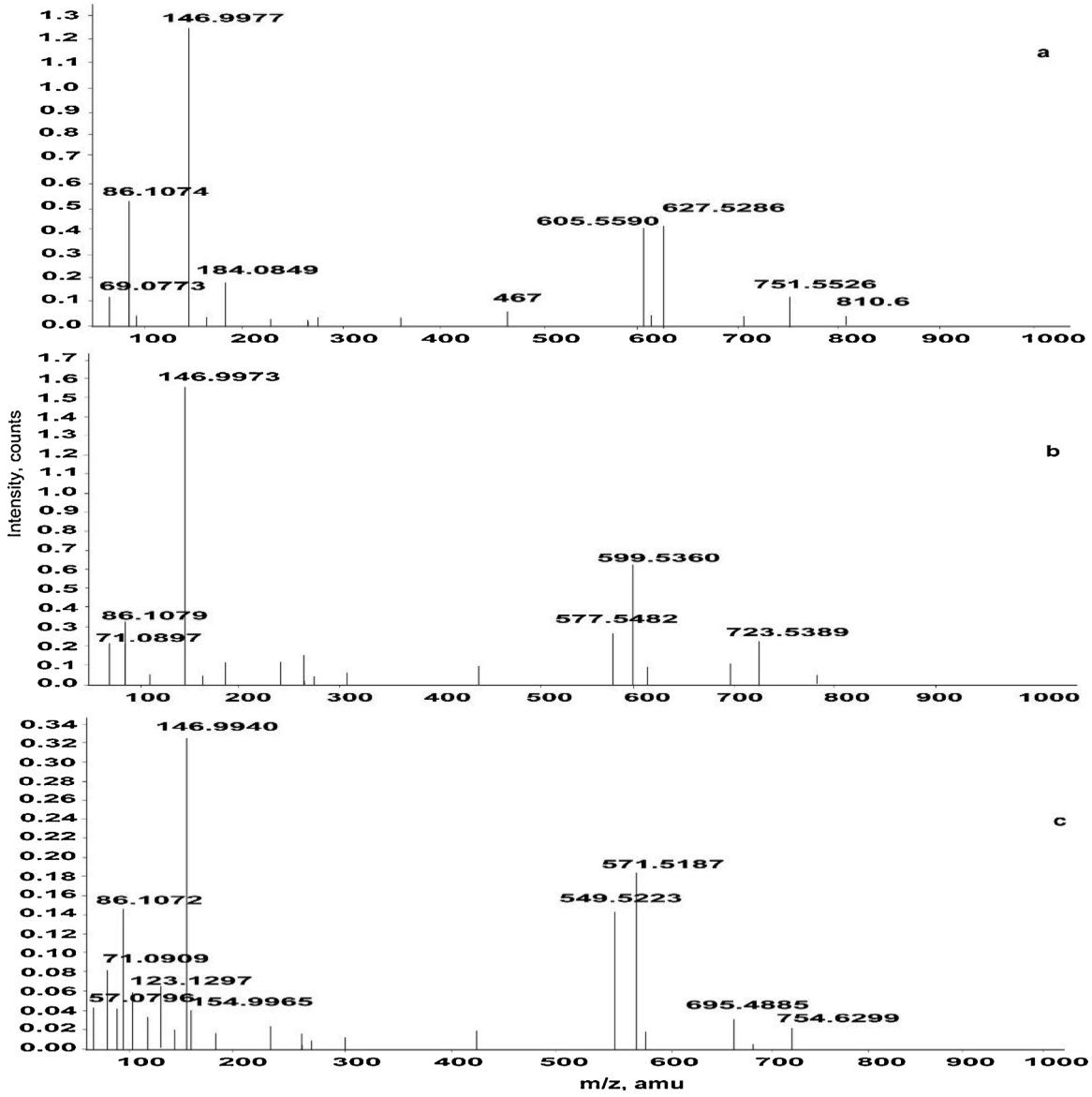

Fig. 8. MS/MS of a) N-2O-acetyl-12 pentadecenoyl acetyl sphingosine phosphorylcholine; b) [M + Na]+ion at *m/z* 782.6 identified as N-9-eicosenoyl- sphinganine phosphorylcholine; and c) sphingomyelin with [M + Na]+ion at *m/z* 754.6 identified as N-9-eicosenoyl- dehydro- sphinganine phosphorylcholine.

linked to original mechanisms of pharmacological activity. The present investigation of the ESI spectrum unveiled intense signals for sodiated molecular ions $[M + Na]^+$ of sphingomyelins identified as *N*-2-O-Acetyl-12 pentadecenoyl sphingosine phosphorylcholine (3, *m/z* 810), N-9-eicosenoyl- sphinganine phosphocholine (4, *m/z* 782). The present study was supported by the ESI-MS of the metabolic extract of hemolymph of crab *H. araneus* shows cluster of peaks in the region *m/z* 445 to *m/z* 491 due to lysoglycerolipids/glycerides and a cluster of signals between *m/z* 216 and 246, due to fatty acids/esters.

In the current study the proton NMR range of the sphingolipid segment displayed signals at δ 5.36 and 5.35 for the unsaturation and δ4.32, 4.14, 3.96, 3.72, 3.48, 3.26 for methine and methylene protons next to oxygen/nitrogen. Similarly the ^{1}HNMR spectrum of the crab *H. araneus* was typical of lipids with special reference to fatty acids and glycerolipids. Clinical use of antimicrobial lipids was suggested many years ago by several authors who emphasized the relative lack of toxicity of antimicrobial lipids from natural sources. However, no pharmaceutical products containing lipids as active compounds have as yet been approved for clinical use as prophylactic or therapeutic drugs.

In the present examination the PHG of sphingolipid with $[M + Na]^+$ at *m/z* 782 was deduced to be phosphocholine on the basis of neutral loss of trimethyl amine/ PC moiety from the molecule (fragments at *m/z* 723/599). In addition, other Sphingolipid metabolismitesbears are potential valuable targets for cancer therapy since sphingolipids are involved in important cellular functions (Jr, 2011). The past decade has seen a dramatic increase in the number of anticancer lead compounds from diverse marine life enter human clinical trials. This has occurred in part during a period of some retrenchment in the field of natural products in general and may cause some to rethink the wisdom of prematurely departing from this highly productive pursuit (Mayer et al., 2010). Nevertheless, it is useful to consider the evolution of the field of marine natural products drug discovery in this context as it may help to identify future directions which will be even more successful.

5. Conclusion

The current investigation tests hemolymph from the marine crab *D. dehaani* for anti-cancer effects while the sphingolipids in the hemolymph were characterized using NMR and ESI-MS. A safe and more

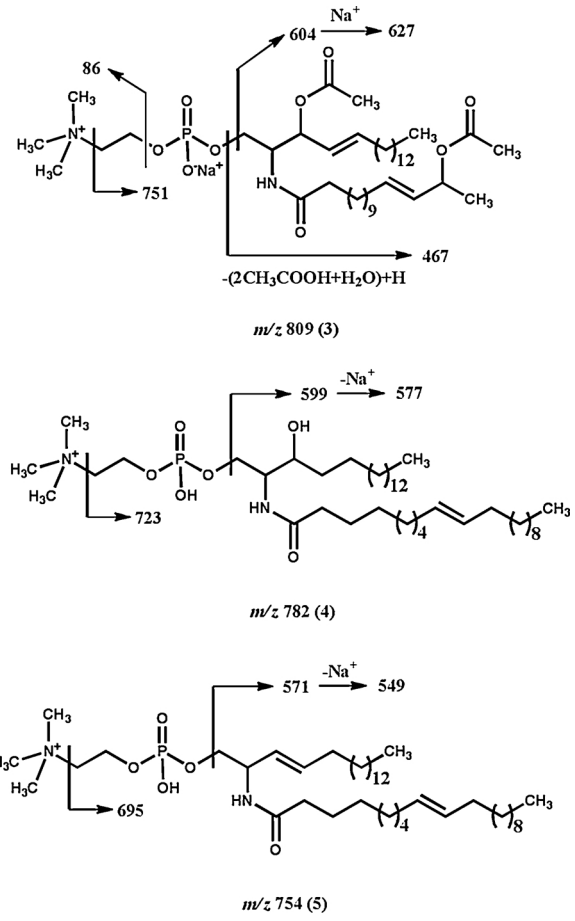

Fig. 9. a) N-2O-Acetyl-12pentadecenoyl phosphorylcholine (*m/z* 809); b) N-9-eicosenoyl- sphinganine phosphocholine (*m/z* 782); c) N-9-eicosenoyl-dehydro-sphinganine phosphocholine (*m/z* 754).

effective natural anti-cancer compound is a challenge to the pharmacological industries, especially with the increased range of cancer throughout world, a safe and more effective natural anti-cancer compound would be beneficial. Hence the anti-cancer potential effects of the brachyuran crab *D. dehaani* hemolymph reported here suggest that its potential is remarkable. Further investigation is warranted. We analyzed the sphingolipid composition of the hemolymph components of which may play an important role in the anti-cancer activity.

Funding

This work was supported by the Department of Biotechnology (BT/PR5769/AAQ/3/597/2012), Government of India.

Conflict of interest

There is no conflict of interest between the authors.

References

Abdel-Mawla, A.A., Fadali, G.A., Youssef, E.A., Eliwa, H.E., 2013. Induction of hepatocellular carcinoma in mice and the role of melatonin. J. Basic Appl. Zool. 66, 206–222. https://doi.org/10.1016/j.jobaz.2012.12.004.

Ahmed, H.H., Shousha, W.G., El-mezayen, H.A., Ismaiel, N.N., Mahmoud, N.S., 2013. In Vivo Antitumor Potential of Carvacrol Against Hepatocellular Carcinoma in Rat Model. World J. Pharm. Pharm. Sci. 2367–2396.

Ali, F., Naz, F., Jyoti, S., Siddique, Y.H., 2014. Mutation research / genetic toxicology and environmental mutagenesis protective effect of apigenin against n -nitrosodiethylamine (NDEA) -induced hepatotoxicity in albino rats. Mutat. Res. Genet. Toxicol. Environ. Mutagen. 767, 13–20. https://doi.org/10.1016/j.mrgentox.2014.04.006.

Antonopoulou, S., Oikonomou, A., Karantonis, H.C., Fragopoulou, E., Pantazidou, A., 2002. From Scytonema Julianum (Cyanobacteria), vol. 293. pp. 287–293.

Arul, D., Subramanian, P., 2013. Bioch emical and biophysical research com munications inhibitory effect of naringenin (citrus flavonone) on N -nitrosodiethylamine induced hepatocarcinogenesis in rats. Biochem. Biophys. Res. Commun. 434, 203–209. https://doi.org/10.1016/j.bbrc.2013.03.039.

Atkinson, J., Harroun, T., Wassall, S.R., Stillwell, W., Katsaras, J., 2010. The location and behavior of α-tocopherol in membranes. Mol. Nutr. Food Res. 54, 641–651. https://doi.org/10.1002/mnfr.200900439.

Ayyad, S.E.N., Bahaffi, S.O.S., Hashish, N.E., 2009. Isolation and structure determination of the biologically active sphingolipids from marine sponge Haliclona species. Nat. Prod. Res. 23, 44–50. https://doi.org/10.1080/14786410701768246.

Balamurugan, K., Karthikeyan, J., 2012. Evaluation of luteolin in the prevention of N-nitrosodiethylamine-induced hepatocellular carcinoma using animal model system. Indian J. Clin. Biochem. 27, 157–163. https://doi.org/10.1007/s12291-011-0166-7.

Chen, P., 2003. Electrospray ionization tandem mass spectrometry in high-throughput screening of homogeneous catalysts. Angew. Chem. Int. Ed. 42, 2832–2847. https://doi.org/10.1002/anie.200200560.

De Luca, T., Morré, D.M., Morré, D.J., 2010. Reciprocal relationship between cytosolic NADH and ENOX2 inhibition triggers sphingolipid-induced apoptosis in HeLa cells. J. Cell. Biochem. 110, 1504–1511. https://doi.org/10.1002/jcb.22724.

Divya, M., Vaseeharan, B., Anjugam, M., Iswarya, A., Karthikeyan, S., Velusamy, P., Govindarajan, M., Alharbi, N.S., Kadaikunnan, S., Khaled, J.M., Vágvölgyi, C., 2018. Phenoloxidase activation, antimicrobial, and antibiofilm properties of β-glucan binding protein from Scylla serrata crab hemolymph. Int. J. Biol. Macromol. 114, 864–873. https://doi.org/10.1016/j.ijbiomac.2018.03.159.

Dmitrenok, A.S., Radhika, P., Anjaneyulu, V., Subrahmanyam, S., Subba Rao, P.V., Dmitrenok, P.S., Boguslavsky, V.M., 2003. New lipids from the soft corals of the Andaman Islands. Russ. Chem. Bull. 52, 1868–1872. https://doi.org/10.1023/A:1026089612129.

Fox, T.E., Finnegan, C.M., Blumenthal, R., Kester, M., 2006. The clinical potential of sphingolipid-based therapeutics. Cell. Mol. Life Sci. 63, 1017–1023. https://doi.org/10.1007/s00018-005-5543-z.

García-Barros, M., Coant, N., Truman, J.P., Snider, A.J., Hannun, Y.A., 2014. Sphingolipids in colon cancer. Biochim. Biophys. Acta Mol. Cell Biol. Lipids 1841, 773–782. https://doi.org/10.1016/j.bbalip.2013.09.007.

Gowda, N.M., Goswami, U., Islam Khan, M., 2008. T-antigen binding lectin with anti-bacterial activity from marine invertebrate, sea cucumber (Holothuria scabra): Possible involvement in differential recognition of bacteria. J. Invertebr. Pathol. 99, 141–145. https://doi.org/10.1016/j.jip.2008.04.003.

Hoshida, Y., Fuchs, B.C., Bardeesy, N., Baumert, T.F., Chung, R.T., 2014. Pathogenesis and prevention of hepatitis C virus-induced hepatocellular carcinoma. J. Hepatol. 61, S79–S90. https://doi.org/10.1016/j.jhep.2014.07.010.

Jayanthi, S., Ishwarya, R., Anjugam, M., Iswarya, A., Karthikeyan, S., Vaseeharan, B., 2017. Purification, characterization and functional analysis of the immune molecule lectin from the haemolymph of blue swimmer crab Portunus pelagicus and their antibiofilm properties. Fish Shellfish Immunol. 62, 227–237. https://doi.org/10.1016/j.fsi.2017.01.019.

Jr, A.M., 2011. Sphingolipid and glycosphingolipid metabolic pathways in the era of sphingolipidomics. Chem. Rev. 111, 6387–6422.

Karthick, C., Periyasamy, S., Jayachandran, K.S., Anusuyadevi, M., 2016. Intrahippocampal Administration of Ibotenic Acid Induced Cholinergic Dysfunction via NR2A/NR2B Expression: Implications of Resveratrol against Alzheimer Disease Pathophysiology. Front. Mol. Neurosci. 9, 1–16. https://doi.org/10.3389/fnmol.2016.00028.

Khotimchenko, S.V., Vas'kovsky, V.E., 2004. An inositol-containing sphingolipid from the red alga Gracilaria verrucosa. Russ. J. Bioorganic Chem. 30, 168–171. https://doi.org/10.1023/B:RUBI.0000023103.14189.27.

Linhart, K., Bartsch, H., Seitz, H.K., 2014. The role of reactive oxygen species (ROS) and cytochrome P-450 2E1 in the generation of carcinogenic etheno-DNA adducts. Redox Biol. 3, 56–62. https://doi.org/10.1016/j.redox.2014.08.009.

Mayer, A.M.S., Glaser, K.B., Cuevas, C., Jacobs, R.S., Kem, W., Little, R.D., McIntosh, J.M., Newman, D.J., Potts, B.C., Shuster, D.E., 2010. The odyssey of marine pharmaceuticals: a current pipeline perspective. Trends Pharmacol. Sci. 31, 255–265. https://doi.org/10.1016/j.tips.2010.02.005.

Morales, A., Lee, H., Goñi, F.M., Kolesnick, R., Fernandez-Checa, J.C., 2007. Sphingolipids and cell death. Apoptosis 12, 923–939. https://doi.org/10.1007/s10495-007-0721-0.

Padrón, J.M., 2006. Sphingolipids in Anticancer Therapy. pp. 755–770.

Piana, G., Trinquart, L., Meskine, N., Barrau, V., Van Beers, B., Vilgrain, V., 2011. New MR imaging criteria with a diffusion-weighted sequence for the diagnosis of hepatocellular carcinoma in chronic liver diseases. J. Hepatol. 55, 126–132. https://doi.org/10.1016/j.jhep.2010.10.023.

Pitson, S.M., 2011. Regulation of sphingosine kinase and sphingolipid signaling. Trends Biochem. Sci. 36, 97–107. https://doi.org/10.1016/j.tibs.2010.08.001.

Ponnusamy, S., Meyers-Needham, M., Senkal, C.E., Saddoughi, S.A., Sentelle, D., Selvam, S.P., Salas, A., Ogretmen, B., 2010. Sphingolipids and cancer: ceramide and sphingosine-1-phosphate in the regulation of cell death and drug resistance. Future Oncol. 6, 1603–1624. https://doi.org/10.2217/fon.10.116.

Ramakrishnan, G., Elinos-Báez, C.M., Jagan, S., Augustine, T.A., Kamaraj, S., Anandakumar, P., Devaki, T., 2008. Silymarin downregulates COX-2 expression and attenuates hyperlipidemia during NDEA-induced rat hepatocellular carcinoma. Mol. Cell. Biochem. 313, 53–61. https://doi.org/10.1007/s11010-008-9741-5.

Reis, A., Domingues, P., Ferrer-Correia, A.J.V., Domingues, M.R.M., 2004. Tandem spectrometry of intact oxidation products of diacylphosphatidylcholines: Evidence for the occurrence of the oxidation of the phosphocholine head and differentiation of

isomers. J. Mass Spectrom. 39, 1513–1522. https://doi.org/10.1002/jms.751.
Rekha, R., Vaseeharan, B., Ishwarya, R., Anjugam, M.S., Alharbi, N., Kadaikunnan, S., Khaled, J.M., Al-anbr, M.N., Govindarajan, M., 2018. Searching for crab-borne antimicrobial peptides: Crustin from Portunus pelagicus triggers biofilm inhibition and immune responses of Artemia salina against GFP tagged Vibrio parahaemolyticus Dahv2. Mol. Immunol. 101, 396–408. https://doi.org/10.1016/j.molimm.2018.07.024.
Schock, T.B., Stancyk, D.A., Thibodeaux, L., Burnett, K.G., Burnett, L.E., Boroujerdi, A.F.B., Bearden, D.W., 2010. Metabolomic analysis of Atlantic blue crab, Callinectes sapidus, hemolymph following oxidative stress. Metabolomics 6, 250–262. https://doi.org/10.1007/s11306-009-0194-y.
Spiegel, S., Kolesnick, R., 2002. Sphingosine 1-phosphate as a therapeutic agent. Leukemia 16, 1596–1602. https://doi.org/10.1038/sj.leu.2402611.
Sugawara, T., Zaima, N., Yamamoto, A., Sakai, S., Noguchi, R., Hirata, T., 2006. Isolation of sphingoid bases of sea cucumber cerebrosides and their cytotoxicity against human colon cancer cells. Biosci. Biotechnol. Biochem. 70, 2906–2912. https://doi.org/10.1271/bbb.60318.
Symolon, H., Bushnev, A., Peng, Q., Ramaraju, H., Mays, S.G., Allegood, J.C., Pruett, S.T., Sullards, M.C., Dillehay, D.L., Liotta, D.C., Merrill, A.H., 2011. Enigmol: a novel sphingolipid analogue with anticancer activity against cancer cell lines and in vivo models for intestinal and prostate cancer. Mol. Cancer Ther. 10, 648–657. https://doi.org/10.1158/1535-7163.MCT-10-0754.
Trafalis, D.T., Panteli, E.S., Grivas, A., Tsigris, C., Karamanakos, P.N., 2010. CYP2E1 and risk of chemically mediated cancers. Expert Opin. Drug Metab. Toxicol. 6, 307–319. https://doi.org/10.1517/17425250903540238.
Trayssac, M., Hannun, Y.A., Obeid, L.M., 2018. Role of sphingolipids in senescence: implication in aging and age-related diseases. J. Clin. Invest. 128, 2702–2712. https://doi.org/10.1172/JCI97949.
Wu, J., Sun, J., Xue, Y., 2010. Involvement of JNK and P53 activation in G2/M cell cycle arrest and apoptosis induced by titanium dioxide nanoparticles in neuron cells. Toxicol. Lett. 199, 269–276. https://doi.org/10.1016/j.toxlet.2010.09.009.
Yao, Z.H., Qin, Z.F., He, L.L., Wang, X.L., Dai, Y., Qin, L., Gonzalez, F.J., Ye, W.C., Yao, X.S., 2017. Identification, bioactivity evaluation and pharmacokinetics of multiple components in rat serum after oral administration of Xian-Ling-Gu-Bao capsule by ultra performance liquid chromatography coupled with quadrupole time-of-flight tandem mass spectrometry. J. Chromatogr. B Anal. Technol. Biomed. Life Sci. 1041–1042, 104–112. https://doi.org/10.1016/j.jchromb.2016.12.026.
Zhang, K., Showalter, M., Revollo, J., Hsu, F.F., Turk, J., Beverley, S.M., 2003. Sphingolipids are essential for differentiation but not growth in Leishmania. EMBO J. 22, 6016–6026. https://doi.org/10.1093/emboj/cdg584.